Behavioural Brain Research 323 (2017) 47–55

Contents lists available at ScienceDirect

Behavioural Brain Research

journal homepage: www.elsevier.com/locate/bbr

Brain-specific knockin of the pathogenic *Tubb5* E401K allele causes defects in motor coordination and prepulse inhibition

Martin W. Breuss*[,1,2], Andi H. Hansen[1,3], Lukas Landler, David A. Keays*

IMP, Research Institute of Molecular Pathology, Vienna 1030, Austria

ARTICLE INFO

Article history:
Received 25 October 2016
Received in revised form 11 January 2017
Accepted 17 January 2017
Available online 25 January 2017

Keywords:
Tubb5
Tubulinopathies
Microcephaly
Malformations of cortical development
Motor defects
Prepulse inhibition

ABSTRACT

The generation, migration, and differentiation of neurons requires the functional integrity of the microtubule cytoskeleton. Mutations in the tubulin gene family are known to cause various neurological diseases including lissencephaly, ocular motor disorders, polymicrogyria and amyotrophic lateral sclerosis. We have previously reported that mutations in *TUBB5* cause microcephaly that is accompanied by severe intellectual impairment and motor delay. Here we present the characterization of a *Tubb5* mouse model that allows for the conditional expression of the pathogenic E401K mutation. Homozygous knockin animals exhibit a severe reduction in brain size and in body weight. These animals do not show any significant impairment in general activity, anxiety, or in the acoustic startle response, however, present with notable defects in motor coordination. When assessed on the static rod apparatus mice took longer to orient and often lost their balance completely. Interestingly, mutant animals also showed defects in prepulse inhibition, a phenotype associated with sensorimotor gating and considered an endophenotype for schizophrenia. This study provides insight into the behavioral consequences of tubulin gene mutations.

1. Introduction

The mammalian neocortex is the result of sequential developmental processes that encompass the generation, migration, and differentiation of neurons [1,2]. Microtubules are known to play a crucial role in each of these cellular events. During mitosis microtubules mediate the separation of sister chromatids; during neuronal migration they form a cage around the nucleus facilitating its movement; and during differentiation microtubules support the extension of axonal and dendritic processes [3]. The importance of the microtubule cytoskeleton in neurodevelopment is reflected by the discovery that mutations in various tubulin genes result in a spectrum of neurological diseases, including: lissencephaly; polymicrogyria; ocular motor disorders, and amyotrophic lateral sclerosis [4–15]. In humans the tubulin gene family consists of 8 alpha- and 9 beta-isoforms [12]. We have previously reported that mutations in *TUBB5* cause microcephaly with structural brain phenotypes [8,16]. *Tubb5* is expressed at high levels in both progenitors and post-mitotic neurons throughout embryonic development, which is maintained at moderate levels postnatally and in adulthood. Patients with mutations in *TUBB5* present primarily with neurological symptoms including: a reduction in orbitofrontal cortex, dysmorphic basal ganglia, dysplasia of the cerebellar vermis, agenesis of the corpus callosum, ataxia, severe language delay, and intellectual impairment.

We have generated a conditional *Tubb5* knockin mouse model that allows for the replacement of the endogenous allele with the pathogenic E401K mutation in a tissue specific manner [17]. This mouse line phenocopies the reduction in brain size observed in patients, which is associated with the perturbation of cell cycle progression in neuronal progenitors and the induction of p53-dependent apoptosis. Traditionally, mouse models associated with neurodevelopmental disease are subject to detailed characterization of the defective developmental events *in utero* that result in anatomical perturbations in the mature nervous system [18–21]. Frequently, however, the impact of any given mutation on the behavioral repertoire of the animal is overlooked. In our view, this is a glaring oversight, as these models may assist in understanding patient phenotypes and, potentially, provide a measurable parameter that could be used for therapeutic screens. This is particularly important in light of the growing evidence that severe

* Correspondence authors.
E-mail addresses: mbreuss@ucsd.edu (M.W. Breuss), david.keays@imp.ac.at (D.A. Keays).
[1] These authors contributed equally to this project.
[2] Current address: Department of Neurosciences, University of California, San Diego, La Jolla, CA 92093, USA.
[3] Current address: Institute of Science and Technology Austria, Klosterneuburg 3400, Austria.

http://dx.doi.org/10.1016/j.bbr.2017.01.029

neurodevelopmental disorders can be alleviated with therapeutic interventions postnatally [22–25]

Accordingly, we have undertaken a systematic behavioral assessment of our E401K Tubb5 mouse mutant complementing our previous work on this gene [4,8,16,17]. Our battery of tests reveals that homozygous E401K animals have motor coordination defects, mirroring the human phenotype accompanied by an impairment in prepulse inhibition indicative of defects in sensorimotor gating.

2. Materials and methods

2.1. Animal housing and breeding

Mice were maintained on a 12:12 light:dark cycle at a temperature of 22 ± 1 °C with a humidity of 60–70%. Males and females were kept separately with a maximum of five male or six female mice in each cage. Animals had *ad libitum* access to food and water. Experiments were performed in accordance with the Austrian Animal Experiments Act (TVG) and Genetic Engineering Act (GTG) under the license number GZ: 11600/2015/25. Tubb5$^{flE401K/flE401K}$ mice were generated and bred as described before [17].

2.2. MRI

Preparation of mice and generation of MRI images were done as described before [17]. In short, mice were transcardially perfused with 0.9% NaCl and 4% PFA containing 10% ProHance Solution (Bracco Imaging Group, 4002750). Whole heads were than imaged with a 15.2 T Biospec horizontal bore scanner (Bruker BioSpin, Ettlingen, Germany).

2.3. Behavioral testing

All behavioral experiments were performed on sex-matched littermates (n = 7 females and 7 males; total n = 14). Each mouse was subjected to one test per day and littermates were tested on the same day. Tests were performed in the same order for each animal (one test a day), starting at 8 weeks of age. The order of the tests were as follows: open field, elevated plus maze, accelerating rotarod, multiple static rods and the acoustic startle response with prepulse inhibition. The same person conducted all experiments at the same time of the day. Behavioral setups were cleaned with 70% ethanol between tests to avoid extraneous odors.

2.3.1. Open field

The open field test was performed in an enclosed grey PVC arena (40 cm x 40 cm base; 30 cm height). Following placement of a mouse in the corner of the arena while facing the wall, its movement and position were tracked for 5 min using the Anymaze software (Stoelting Co., Wood Dale, IL, USA) [26].

2.3.2. Elevated plus maze

The elevated plus maze consisted of two opposing open arms (29 cm long, 6 cm wide) and two opposing enclosed arms (27 cm long, 6 cm wide, 18 cm height) placed 30 cm above the ground. Following placement of the mouse in the middle facing one of the closed arms its movement and position was tracked for 5 min using the Anymaze software (Stoelting Co., Wood Dale, IL, USA).

2.3.3. Accelerating rotarod

Mice were placed on the beam of the rotarod (Ugo Basile, Italy) facing in the opposite direction relative to the rotation for 1 min at 5 rpm. Subsequently, the rod automatically accelerated to a maximum of 30 rpm over 4 min. The latency before falling was measured up to a maximum of 6 min. Three trials with 1 h intervals were carried out [27]. Animals had not previously been exposed to the rotarod.

2.3.4. Acoustic startle response with prepulse inhibition

The commercially available setup (San Diego Instruments, San Diego, CA, USA) consists of a mouse chamber mounted on an accelerometer inside a soundproof box with a 6 cm speaker that delivers the acoustic stimuli. Following placement inside the chamber, the mouse was allowed to acclimatize 5 min. The acoustic stimuli were delivered at four different intensities (90, 100, 110 and 120 dB) as 40 ms of white noise for a total of 20 times [28]. Subsequent prepulse inhibition testing was performed at two different pre pulses (90 dB and 95 dB) followed by the same 120 dB stimulus. Averaged response from 0 to 120 was used as maximum value. All stimuli were delivered in a pseudorandom order at random intervals ranging from 10 to 20 s. Responses were assembled in arbitrary units and averaged for each startle intensity.

2.3.5. Multiple static rods

The multiple static rods setup consisted of a series of five 60 cm long wooden rods with decreasing width (rod 1:3.3 cm; rod 2:2.7 cm; rod 3:2.1 cm; rod 4:1.4 cm; and rod 5:0.8 cm) mounted perpendicularly to the supporting base that was elevated 60 cm above a cushioned surface [26]. Starting with rod 1, mice were placed on the distal end facing away from the supporting base. Both, latency to turn 180 ° to face the base (orientation time) and the total time until all four paws were placed on the supporting base (time to target) were recorded for a maximum of 180 s. If the mouse fell from one of the rods or turned upside down during the test it was given the maximum score of 180 s [26]. After each individual rod tested mice were returned to the cage to rest.

2.4. Statistical methods and data analysis

Brain weights were compared between genotypes using a one-way ANOVA, with a post-hoc Tukey comparison. For the static rod test, prepulse inhibition test, and rotarod experiments we performed repeated measures ANOVAs using the trial rounds for each mouse as the repeated factor and genotypes as the between subject factor, we also tested for an interaction effect between genotypes and trial round. The open field experiments and the elevated plus maze were analyzed using one-way ANOVA models in order to test for differences between the three genotypes. For all tests a Tukey post-hoc comparison was used to compare genotypes within the ANOVA models, and to assess trial improvement for the rotarod experiments. Where multiple measures were obtained in one experiment, we corrected for multiple testing using a Bonferroni correction. An assessment of sex was initially performed on all datasets, however, we observed no sex effect with the exception of the acoustic startle response (see Table S2 in the online version at DOI: http://dx.doi.org/10.1016/j.bbr.2017.01.029). The acoustic startle response was therefore analyzed using a two-way ANOVA model including sex and genotype for each of the DB levels followed by a Bonferroni correction. All analyses were calculated using Prism 7 for Mac OS X (Version 7.0a).

3. Results

Brain-specific homozygous knockin mice (HOM/+) were generated by interbreeding heterozygous males, carrying the Nestin-Cre transgene, with homozygous females (Fig. 1A–D) [17]. Littermate animals heterozygous for the knockin allele, with and without Nestin-Cre, (HET/+ and HET/-) were also phenotyped. As reported previously, homozygous knockin animals exhibited severe microcephaly (Fig. 1C–E) [17] and further showed a reduction in body

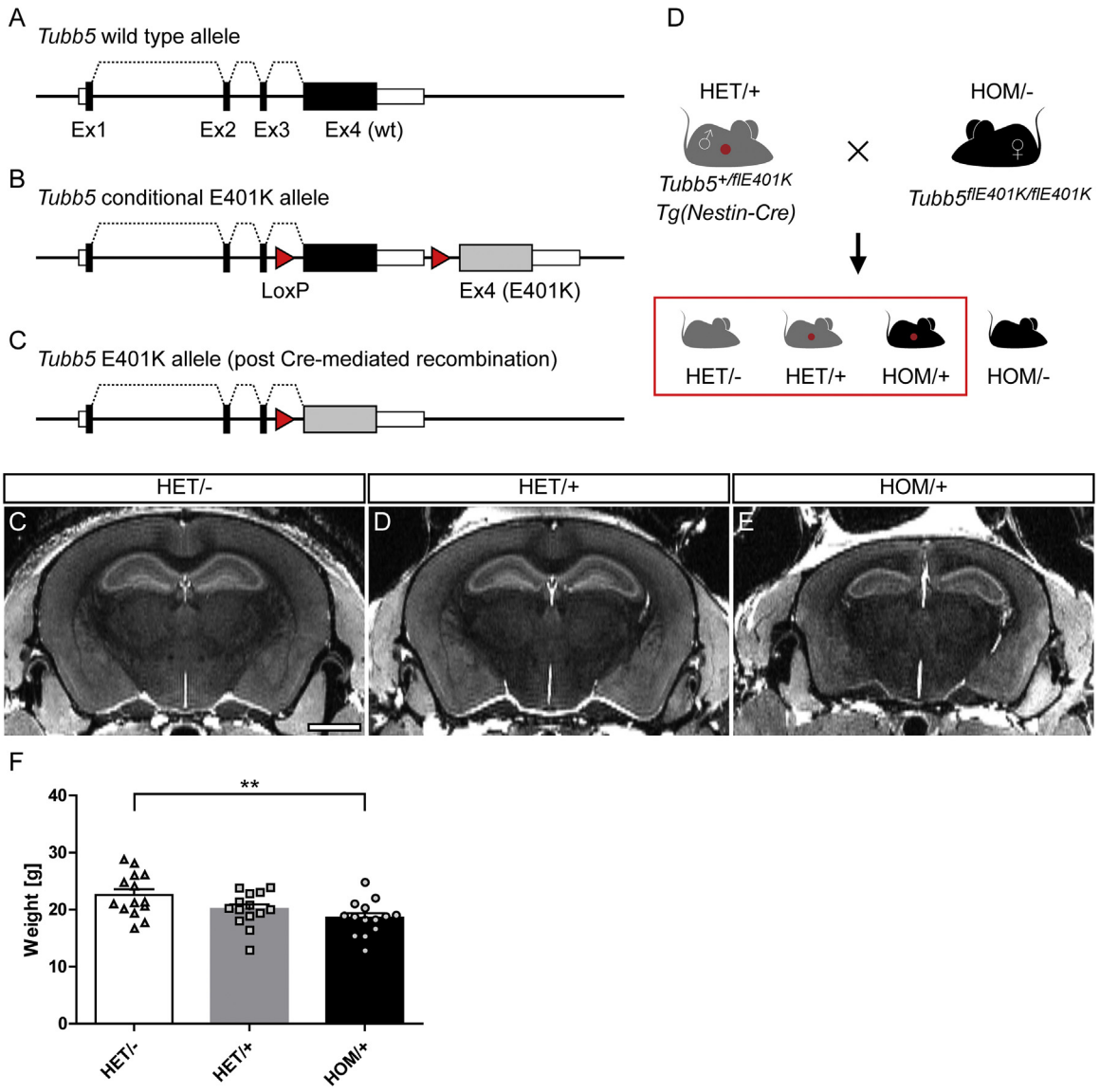

Fig. 1. Tubb5 E401K knockin mice show reduced brain size and body weight. A–C: Schematic of the wild type *Tubb5* locus (A) and the conditional E401 K allele, pre and post Cre-recombination (B and C, respectively). Ex: exon; LoxP: LoxP recombination sites. D: Breeding schematic for the generation of behaviorally assessed mice. Heterozygous E401 K conditional knockin males carrying a Nestin-Cre transgene were interbred with homozygous knockin females. Heterozygous animals without (HET/-), as well as heterozygous and homozygous mice with the Nest-Cre transgene (HET/+ and HOM/+, respectively) were used for the described experiments. C-E: Coronal MRI views of a representative HET/- (C), HET/+ (D), and HOM/+ brain. HOM/+ animals show profound microcephaly. Images are derived from the same data set originally presented in [17]. F: Weight quantification of animals of the indicated genotypes at 10–12 weeks of age. **P < 0.01. Graphs show the individual values as well as the mean ± SEM. n = 14 (7 males; 7 females; sex-matched littermates).

weight (Fig. 1F) ($F(2, 39) = 5.275$, $P = 0.0094$; Tukey post-hoc comparison: HOM/+ vs. HET/-: $P < 0.01$; see Table S1 for a summary of all statistical analyses in the online version at DOI: http://dx.doi.org/10.1016/j.bbr.2017.01.029%20). Animals were submitted to a battery of behavioral tests. In the following order, they were assessed on: the open field; the elevated plus maze; the accelerating rotarod; static rods; and, finally, for sensorimotor gating. We tested a total of 14 littermate trios, which were divided evenly into males (n = 7) and females (n = 7). We did not observe a sex effect for any of the behaviors, except for one sound level when assessing the acoustic startle response (see Table S2 in the online version at DOI: http://dx.doi.org/10.1016/j.bbr.2017.01.029).

The open field test assessed the overall activity of animals, as well as anxiety phenotypes (Fig. 2) [26]. Animals were placed in a square arena and their movement and position was tracked for 5 min. Homozygous knockin mice, did not show any differences in the number of entries into or time spent in the open center or their latency center entry (Fig. 2A-B, E). There was a slight, although non-significant increase in distance covered in the open and peripheral areas during the test, suggesting increased activity (Fig. 2C–D). Consistent with this result mice spent less time immobile (Fig. 2F) (number of entries: $F(2, 39) = 0.967$, adjusted $P > 0.99$; open time overall: $F(2, 39) = 0.014$, adjusted $P > 0.99$; wall distance: $F(2, 39) = 1.903$, adjusted $P = 0.97$; latency to first entry: $F(2, 39) = 0.4119$, adjusted $P > 0.99$; open distance: $F(2, 39) = 0.8788$, adjusted $P > 0.99$).

The elevated plus maze tested anxiety by contrasting behavior in the open and closed arms of the apparatus (Fig. 3) [26]. In this assay mice were placed in the middle of an elevated cross-shaped platform with two walled and to open arms. Movement and position were then tracked automatically. In general, homozygous knockin animals exhibited a higher ratio of open to closed arm entries indicative of decreased anxiety, however, this result was not significant (Fig. 3A–D) (entries open/closed ratio: $F(2, 39) = 3689$, adjusted

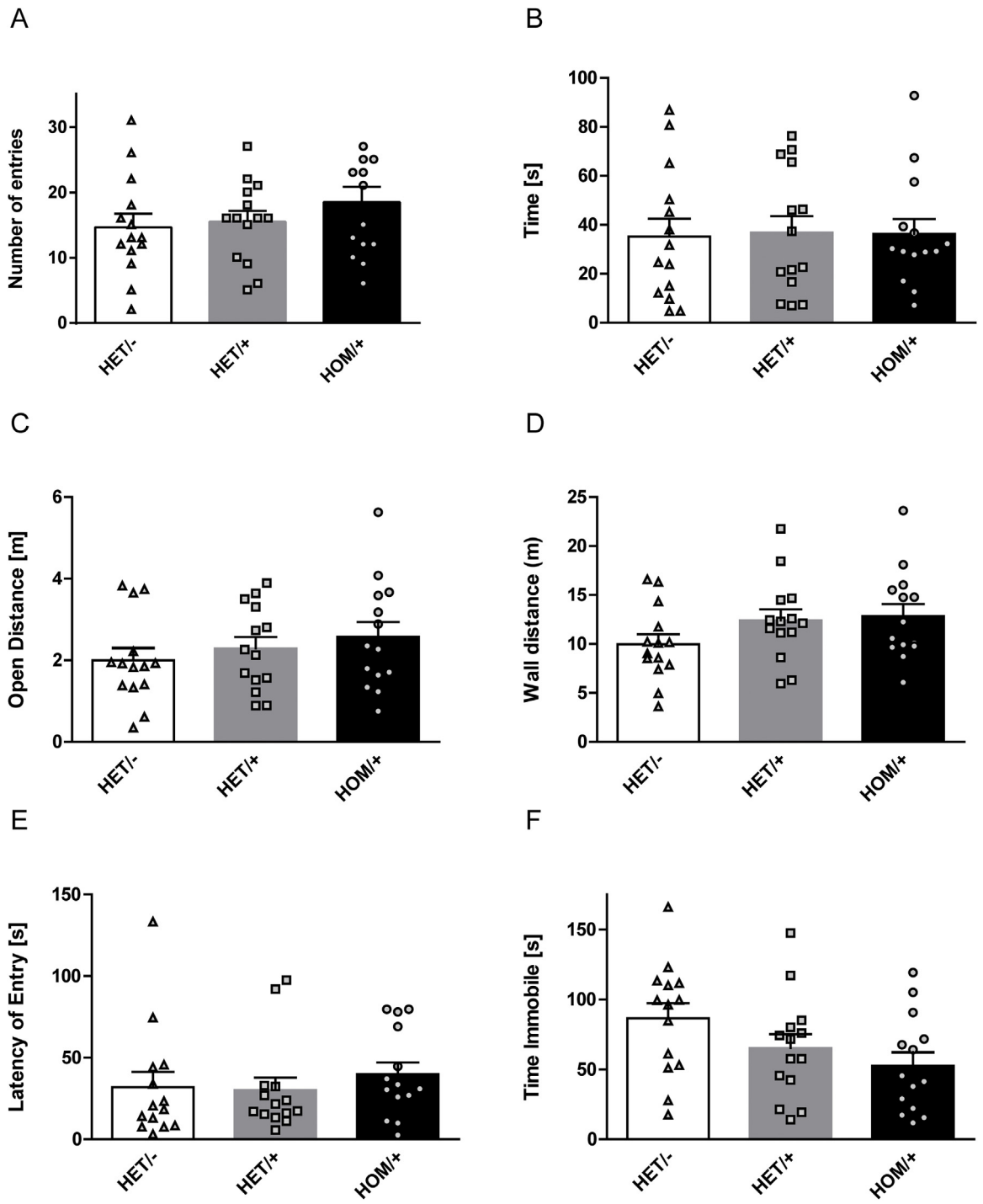

Fig. 2. E401K knockin animals do not show behavioral abnormalities in an open field test. A-F: Quantification of several parameters measured during the open field test. Shown are the number of entries into the open field (A), the time spent in the open field (B), the distance covered by an individual mouse in the open field (C) and along the wall (D), the latency of first entry into the open field (E), and the time a mouse remained immobile (F). Graphs show the individual values as well as the mean ± SEM. n = 14 (7 males; 7 females; sex-matched littermates).

P = 0.103). Nor were there significant differences when comparing the ratios of distance covered in the open versus closed arms, time spent in open versus closed arms, or the total distance travelled (Fig. 3A–D) (distance open/closed ratio: $F(2, 39) = 0.7739$, adjusted $P > 0.99$; time open/closed ratio: $F(2, 39) = 0.0865$, adjusted $P > 0.99$; total distance covered: $F(2, 39) = 0.758$, adjusted $P > 0.99$).

The accelerating rotarod was employed to test balance and motor coordination (Fig. 4) [26]. In this test, animals were positioned on a slowly accelerating rod in three separate trials and the latency to fall was recorded. Overall, we did not observe any significant differences when comparing homozygous knockin mice with their heterozygous and control littermates (Fig. 4) ($F(2, 39) = 1.987$, $P = 0.151$). This may be related to the reduced weight of homozygous knockin animals (Fig. 1F). We did observe a noticeable improvement in the performance of control animals over three trials, that was not evident in heterozygous or homozygous mutants (Tukey post-hoc comparison: HET/-; Trial 1 vs Trial 3; $P = 0.001$). We complemented this analysis with an assessment on

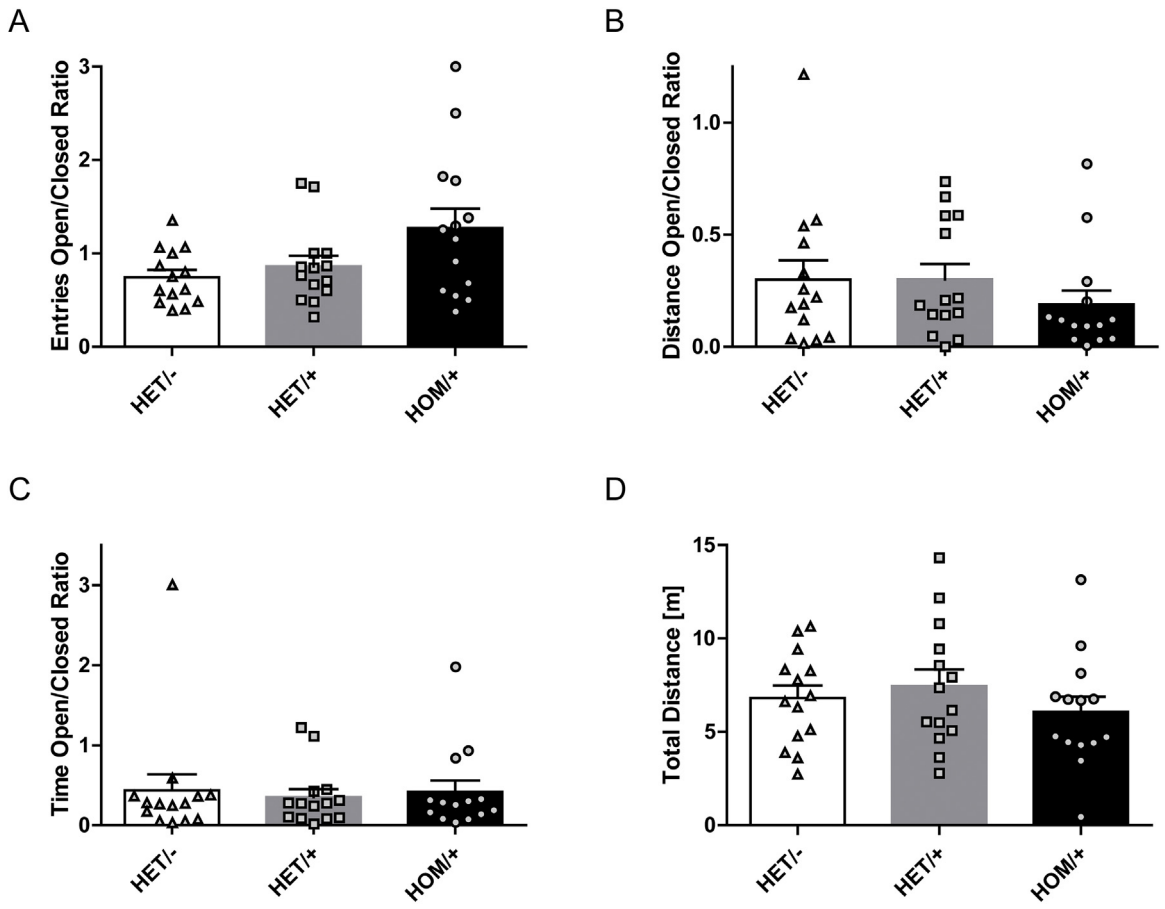

Fig. 3. Fear behavior assessed in an elevated plus maze is unaffected by E401K knockin. A-C: Quantification of the ratio of open and closed entrances (A), the ratio of distance covered in the open and closed arms (B), the ratio of time spent in the open and closed arms (C), and the total distance covered (D). Graphs show the individual values as well as the mean ± SEM. n = 14 (7 males; 7 females; sex-matched littermates).

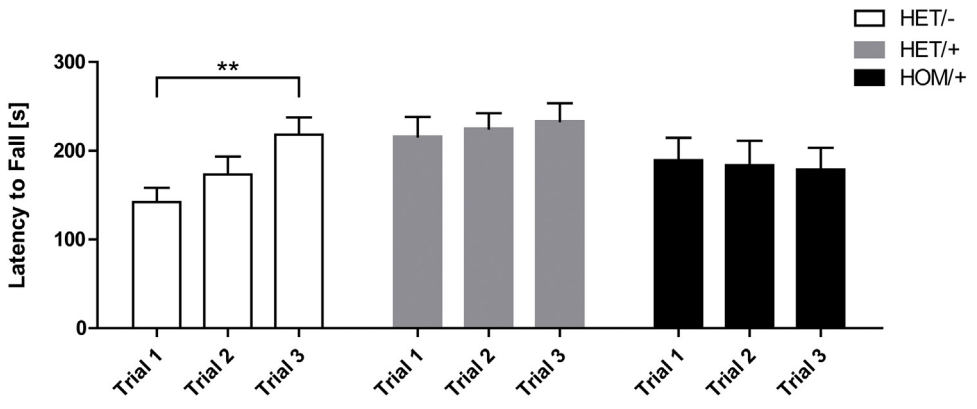

Fig. 4. Analysis of E401K knockin mice on the rotarod. Quantification of the latency to fall of the rotarod for the individual animals in three replicate trials. While overall there is no significant differences between genotypes, HET/- animals show an improvement in trial performance that is not evident in HET/+ and HOM/+ animals. **P < 0.01. Graphs show mean ± SEM. n = 14 (7 males; 7 females; sex-matched littermates).

the multiple static rods (Fig. 5) [26]. Here, mice were placed on five rods with decreasing diameter facing away from a safe platform. For each rod the time to orient towards the target, and the total time taken to reach the target were recorded. This setup revealed a significant difference when comparing genotypes (orientation time: $F(2, 39) = 11.21$, adjusted $P = 0.0002$; target time: $F(2, 39) = 10.96$, adjusted $P = 0.0004$; Tukey post-hoc comparison: orientation time: HOM/+ vs. HET/+: adjusted $P = 0.004$, HOM/+ vs. HET/-: adjusted $P = 0.0004$; target time: HOM/+ vs. HET/+: adjusted $P = 0.006$, HOM/+ vs. HET/-: adjusted $P = 0.0004$). Both, orientation (Fig. 5A) and target time (Fig. 5B), were significantly longer in the homozygous knockin animals in comparison to their heterozygous and control littermates. Heterozygous animals did, in general take longer to orient and reach the target than controls, however this was not significantly different (orientation time: HET/+ vs. HET/-: adjusted $P > 0.99$; target time: HET/+ v HET/-: adjusted $P > 0.99$). Most strikingly, mutant animals did not exhibit any improved performance in orientation time following exposure to the setup on the first rod.

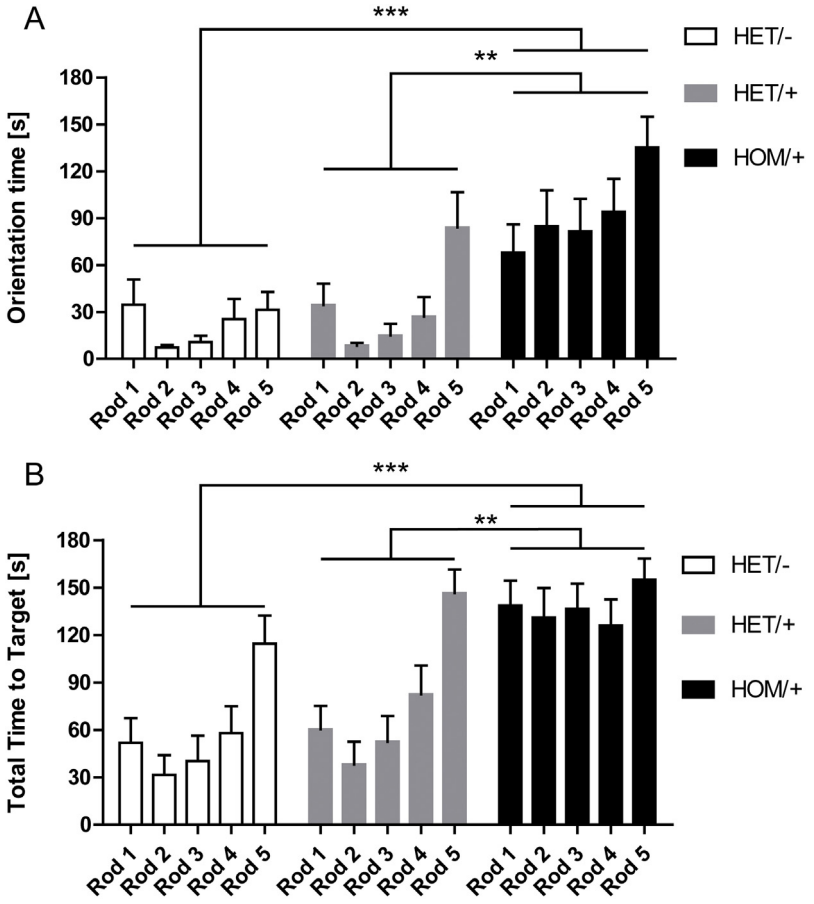

Fig. 5. E401K knockin impairs motor coordination assessed by a multiple static rods. A-B: Quantifications for orientation (A) and target time (B) needed for the rods of descending diameter, indicated with Rod 1–5. $^{**}P < 0.01$, $^{***}P < 0.001$. Graphs show mean ± SEM. n = 14 (7 males; 7 females; sex-matched littermates).

Finally, we tested the acoustic startle response to assess sensorimotor gating (Fig. 6A) and prepulse inhibition which relates to the filtering of information and is considered to be an endophenotype for schizophrenia (Fig. 6B) [28,29]. Analysis of the startle response to 90 dB, 100 dB, 110 dB, and 120 dB revealed no significant difference between genotypes (Fig. 6A) (90 dB: $F(2,36) = 0.967$, $P > 0.99$; 100 dB: $F(2,36) = 0.409$, $P > 0.99$; 110 dB: $F(2,36) = 0.572$, $P > 0.99$; 120 dB: $F(2,36) = 0.563$, $P > 0.99$). We did observe a sex effect for 110 dB ($F(1,36) = 8.03$, $P < 0.05$), but no interaction between sex and genotype ($F(2,36) = 0.166$, $P > 0.99$). Analysis of prepulse inhibition when presented with a 90 dB and 95 dB prepulse to a 120 dB stimulus revealed a significant impairment in HOM/+ animals (Fig. 6B) ($F(2, 39) = 3.797$, $P = 0.03$; Tukey post-hoc comparison: 90dB–120 dB: HOM/+ vs. HET/-: $P = 0.01$).

4. Discussion

While behavioral characterization of mouse models of autism spectrum disorders and schizophrenia have been frequent, only a few mouse models with structural brain phenotypes have undergone behavioral assessment [30–34]. Although a number of mouse models for primary microcephaly exist (e.g. *Mcph1*, *Cdk5rap2*, *Wdr62*, and *Aspm*), to our knowledge none of these animals have not been subject to behavioral assessment [18–21]. A mouse model for Glut-1 deficiency syndrome, a disease characterised by seizures, acquired microcephaly and low glucose levels in the cerebrospinal fluid has been investigated [35]. It has been reported that Glut-1 knockout animals exhibit impaired motor performance, falling from the rotarod more frequently accompanied by defects in beam walking. Similarly, we observed a severe defect in our E401K mutant animals when assessing their motor co-ordination on the static rods apparatus. One of the most striking phenotypes observed in *TUBB5* patients is their delay in motor development and coordination [5,8]. This phenotype, which is often described in patients with tubulin gene mutations, may be associated with basal ganglia abnormalities and hypoplasia of the cerebellum [5,8,12,36–38]. Reflecting this, the E401 K knockin mice present with a volumetric reduction in both brain regions [17].

Surprisingly, we also observed defects in sensorimotor gating, specifically in prepulse inhibition, impairments of which have been described in mouse models of schizophrenia [39,40]. For instance, an ENU-induced mouse model for the schizophrenia gene *Disc1* shows a robust defect in this assay [41,42]. Likewise, various mutants interfering with NMDA receptor function impair prepulse inhibition [41]. Although the interpretation of such phenotypes can be difficult, dysregulation of TUBB5 expression has been correlated with schizophrenia previously [43,44]. Moreover, brain size decrease in general has been associated with this disorder [45]. Given these connections, it would be interesting to test whether drugs that improve prepulse inhibition phenotypes in schizophrenia mouse models could evoke the same response in the E401K knockin mice [46]. It is interesting to note that the *Jenna* mice, which harbor a S140G mutation in *Tuba1a* exhibit a marked increase in locomotor activity and an exaggerated acoustic startle response which we did not observe in our E401K animals [11,28]. This result suggests that different neuronal circuits are likely perturbed in these mouse lines, perhaps reflecting the functional properties or expression patterns of these different tubulin isoforms.

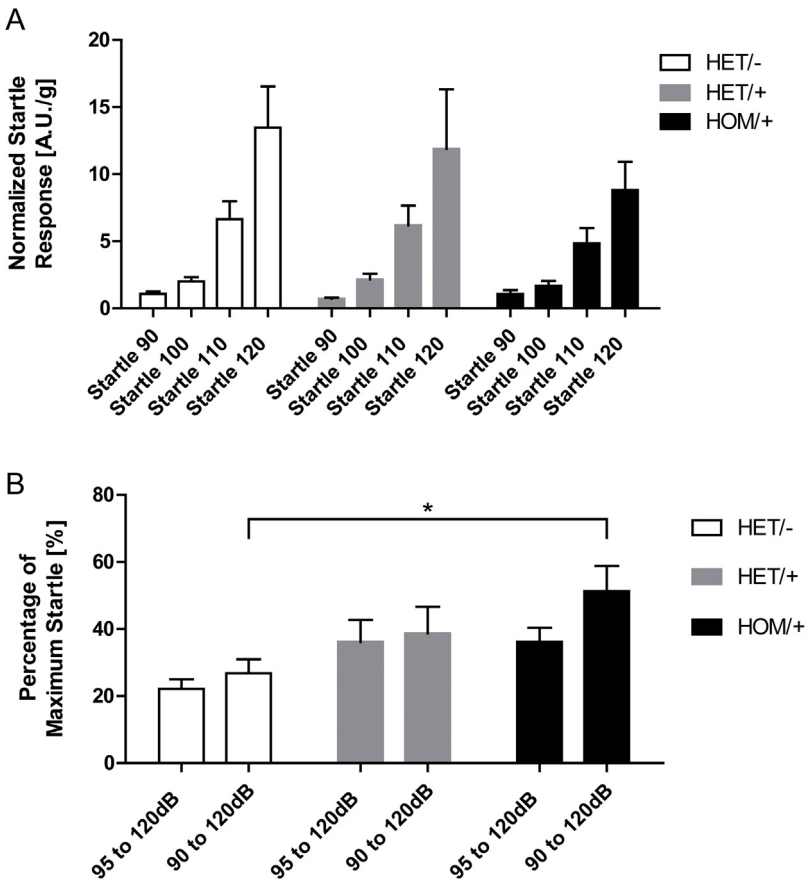

Fig. 6. E401K knockin does not alter the acoustic startle response, but impairs prepulse inhibition. A: Quantification of the weight-normalized startle response for the indicated sound intensities (measured in dB). B: Quantification of the relative startle response to a 120 dB sound following a prepulse of the indicated intensity. *P < 0.05. Graphs show mean ± SEM. n = 14 (7 males; 7 females; sex-matched littermates).

It is known that structural brain abnormalities, such as microcephaly, originate from defects in basic biological processes *in utero*. The extent to which defects in postnatal neuronal function contributes to a patient's phenotype is often difficult to ascertain. Given that *TUBB5* is expressed at moderate levels directly after birth and in the adult brain, it is conceivable that dysfunction postnatally might exacerbate any anatomical or behavioral deficits. Consequently, there is a window in which it might be possible to intervene with some therapeutic benefit. For instance, it has been demonstrated that postnatal expression of Dcx in a rat model for subcortical band heterotopia can rescue the phenotype [47]. Similarly, Novarino and colleagues have described a metabolically induced autism disorder, for which treatment in adult mice can improve the behavioral defects [22]. Postnatal interventions are also being explored for the treatment of human patients with neurofibromatosis type I and tuberous sclerosis [24,25].

Might a similar approach be successful with respect to TUBB5? Might we be able to alleviate the disease state by application of a drug that limits apoptotic cell death, or alternatively drive expression of another, closely related tubulin isoform? Drugs with the potential to inhibit apoptosis are of great interest for neurodegenerative disorders or treatment of acute cell death due to insult, such as stroke induced hypoxia [48]. Although inhibition of the apoptotic cascade is possible, alternative pathways often ensure that cell death is only delayed rather than prevented. A recent study by Jiang and colleagues, however, reports the discovery of a small molecule that protects the integrity of the electron transport chain in mitochondria, limiting apoptosis [49]. Preliminary tests in a mouse model of neurodegeneration were promising and make it a viable compound to test in mouse models of microcephaly that are driven by apoptotic cell death.

The extent to which different tubulin isoforms are functional redundant is not clear, however, it may also be beneficial to induce overexpression of another tubulin isoform postnatally (e.g. *TUBB2A* or *TUBB2B*) [50]. In instances where heterozygous *TUBB5* mutations act by loss of function compounds that increase expression of *TUBB5* itself may also be of utility. The existence of different tubulin GFP-reporter lines (e.g. *Tg(Tubb5-GFP)*) could be used to assess the ability of compounds to upregulate tubulin expression providing avenues to test these ideas [8,17,50].

5. Conclusions

Taken together, we have described the behavioral characterization of the Tubb5 E401K knockin model and discovered defects in motor control and, unexpectedly, prepulse inhibition of the acoustic startle response. Our study provides quantitative behavioral readouts that could be used to assess the utility of therapeutic interventions for *TUBB5* associated neurological disease.

Acknowledgements

We wish to acknowledge the IMP-IMBA transgenic services and the animal attendants for their assistance. MRI acquisition was performed by the Preclinical Imaging Facility of the Campus Science Support Facilities GmbH (CSF). We want to further thankanja Fritz and Marion C. Salzer for excellent technical assistance with mouse colony maintenance and experiments. We are indebted to

Boehringer Ingelheim and the Austrian Science Fund (FWF) for funding this research [I914, P21092].

References

[1] M. Kuijpers, C.C. Hoogenraad, Centrosomes, microtubules and neuronal development, Mol. Cell. Neurosci. 48 (4) (2011) 349–358.
[2] R. Ayala, T. Shu, L.H. Tsai, Trekking across the brain: the journey of neuronal migration, Cell 128 (1) (2007) 29–43.
[3] R. Romaniello, F. Arrigoni, M.T. Bassi, R. Borgatti, Mutations in alpha- and beta-tubulin encoding genes: implications in brain malformations, Brain Dev. 37 (3) (2015) 273–280.
[4] M. Isrie, M. Breuss, G. Tian, A.H. Hansen, F. Cristofoli, J. Morandell, Z.A. Kupchinsky, A. Sifrim, C.M. Rodriguez-Rodriguez, E.P. Dapena, K. Doonanco, N. Leonard, F. Tinsa, S. Moortgat, H. Ulucan, E. Koparir, E. Karaca, N. Katsanis, V. Marton, J.R. Vermeesch, E.E. Davis, N.J. Cowan, D.A. Keays, H. Van Esch, Mutations in either TUBB or MAPRE2 cause circumferential skin creases kunze type, Am. J. Hum. Genet. 97 (6) (2015) 790–800.
[5] N. Bahi-Buisson, K. Poirier, F. Fourniol, Y. Saillour, S. Valence, N. Lebrun, M. Hully, C.F. Bianco, N. Boddaert, C. Elie, K. Lascelles, I. Souville, L.I.-T. Consortium, C. Beldjord, J. Chelly, The wide spectrum of tubulinopathies: what are the key features for the diagnosis? Brain 137 (Pt 6) (2014) 1676–1700.
[6] B.N. Smith, N. Ticozzi, C. Fallini, A.S. Gkazi, S. Topp, K.P. Kenna, E.L. Scotter, J. Kost, P. Keagle, J.W. Miller, D. Calini, C. Vance, E.W. Danielson, C. Troakes, C. Tiloca, S. Al-Sarraj, E.A. Lewis, A. King, C. Colombrita, V. Pensato, B. Castellotti, J. de Belleroche, F. Baas, A.L. ten Asbroek, P.C. Sapp, D. McKenna-Yasek, R.L. McLaughlin, M. Polak, S. Asress, J. Esteban-Perez, J.L. Munoz-Blanco, M. Simpson, S. Consortium, W. van Rheenen, F.P. Diekstra, G. Lauria, S. Duga, S. Corti, C. Cereda, L. Corrado, G. Soraru, K.E. Morrison, K.L. Williams, G.A. Nicholson, I.P. Blair, P.A. Dion, C.S. Leblond, G.A. Rouleau, O. Hardiman, J.H. Veldink, L.H. van den Berg, A. Al-Chalabi, H. Pall, P.J. Shaw, M.R. Turner, K. Talbot, F. Taroni, A. Garcia-Redondo, Z. Wu, J.D. Glass, C. Gellera, A. Ratti, R.H. Brown Jr., V. Silani, C.E. Shaw, J.E. Landers, Exome-wide rare variant analysis identifies TUBA4A mutations associated with familial ALS, Neuron 84 (2) (2014) 324–331.
[7] C. Simons, N.I. Wolf, N. McNeil, L. Caldovic, J.M. Devaney, A. Takanohashi, J. Crawford, K. Ru, S.M. Grimmond, D. Miller, D. Tonduti, J.L. Schmidt, R.S. Chudnow, R. van Coster, L. Lagae, J. Kisler, J. Sperner, M.S. van der Knaap, R. Schiffmann, R.J. Taft, A. Vanderver, A de novo mutation in the beta-tubulin gene TUBB4A results in the leukoencephalopathy hypomyelination with atrophy of the basal ganglia and cerebellum, Am. J. Hum. Genet. 92 (5) (2013) 767–773.
[8] M. Breuss, J. Heng, K. Poirier, G. Tian, X. Jaglin, Z. Qu, A. Braun, T. Gstrein, L. Ngo, M. Haas, N. Bahi-Buisson, M. Moutard, S. Passemard, A. Verloes, P. Gressens, Y. Xie, K.H. Robson, D. Rani, K. Thangaraj, T. Clausen, J. Chelly, N. Cowan, D. Keays, Mutations in the β-tubulin gene TUBB5 cause microcephaly with structural brain abnormalities, Cell Rep. 2 (6) (2012) 1554–1562.
[9] M.A. Tischfield, H.N. Baris, C. Wu, G. Rudolph, L. Van Maldergem, W. He, W.M. Chan, C. Andrews, J.L. Demer, R.L. Robertson, D.A. Mackey, J.B. Ruddle, T.D. Bird, I. Gottlob, C. Pieh, E.I. Traboulsi, S.L. Pomeroy, D.G. Hunter, J.S. Soul, A. Newlin, L.J. Sabol, E.J. Doherty, C.E. de Uzcategui, N. de Uzcategui, M.L. Collins, E.C. Sener, B. Wabbels, H. Hellebrand, T. Meitinger, T. de Berardinis, A. Magli, C. Schiavi, M. Pastore-Trossello, F. Koc, A.M. Wong, A.V. Levin, M.T. Geraghty, M. Descartes, M. Flaherty, R.V. Jamieson, H.U. Moller, I. Meuthen, D.F. Callen, J. Kerwin, S. Lindsay, A. Meindl, M.L. Gupta Jr., D. Pellman, E.C. Engle, Human TUBB3 mutations perturb microtubule dynamics, kinesin interactions, and axon guidance, Cell 140 (1) (2010) 74–87.
[10] X.H. Jaglin, K. Poirier, Y. Saillour, E. Buhler, G. Tian, N. Bahi-Buisson, C. Fallet-Bianco, F. Phan-Dinh-Tuy, X.P. Kong, P. Bomont, L. Castelnau-Ptakhine, S. Odent, P. Loget, M. Kossorotoff, I. Snoeck, G. Plessis, P. Parent, C. Beldjord, C. Cardoso, A. Represa, J. Flint, D.A. Keays, N.J. Cowan, J. Chelly, Mutations in the beta-tubulin gene TUBB2B result in asymmetrical polymicrogyria, Nat. Genet. 41 (6) (2009) 746–752.
[11] D.A. Keays, G. Tian, K. Poirier, G.J. Huang, C. Siebold, J. Cleak, P.L. Oliver, M. Fray, R.J. Harvey, Z. Molnar, M.C. Pinon, N. Dear, W. Valdar, S.D. Brown, K.E. Davies, J.N. Rawlins, N.J. Cowan, P. Nolan, J. Chelly, J. Flint, Mutations in alpha-tubulin cause abnormal neuronal migration in mice and lissencephaly in humans, Cell 128 (1) (2007) 45–57.
[12] M. Breuss, D.A. Keays, Microtubules and neurodevelopmental disease: the movers and the makers, in: L. Nguyen, S. Hippenmeyer (Eds.), Cellular and Molecular Control of Neuronal Migration, Springer, Netherlands, Dordrecht, 2014, pp. 75–96.
[13] J. Hersheson, N.E. Mencacci, M. Davis, N. MacDonald, D. Trabzuni, M. Ryten, A. Pittman, R. Paudel, E. Kara, K. Fawcett, V. Plagnol, K.P. Bhatia, A.J. Medlar, H.C. Stanescu, J. Hardy, R. Kleta, N.W. Wood, H. Houlden, Mutations in the autoregulatory domain of beta-tubulin 4a cause hereditary dystonia, Ann. Neurol. 73 (4) (2013) 546–553.
[14] K. Lohmann, R.A. Wilcox, S. Winkler, A. Ramirez, A. Rakovic, J.S. Park, B. Arns, T. Lohnau, J. Groen, M. Kasten, N. Bruggemann, J. Hagenah, A. Schmidt, F.J. Kaiser, K.R. Kumar, K. Zschiedrich, D. Alvarez-Fischer, E. Altenmuller, A. Ferbert, A.E. Lang, A. Munchau, V. Kostic, K. Simonyan, M. Agzarian, L.J. Ozelius, A.P. Langeveld, C.M. Sue, M.A. Tijssen, C. Klein, Whispering dysphonia (DYT4 dystonia) is caused by a mutation in the TUBB4 gene, Ann. Neurol. 73 (4) (2013) 537–545.
[15] R. Feng, Q. Sang, Y. Kuang, X. Sun, Z. Yan, S. Zhang, J. Shi, G. Tian, A. Luchniak, Y. Fukuda, B. Li, M. Yu, J. Chen, Y. Xu, L. Guo, R. Qu, X. Wang, Z. Sun, M. Liu, H. Shi, H. Wang, Y. Feng, R. Shao, R. Chai, Q. Li, Q. Xing, R. Zhang, E. Nogales, L. Jin, L. He, M.L. Gupta Jr., N.J. Cowan, L. Wang, Mutations in TUBB8 and human oocyte meiotic arrest, N. Engl. J. Med. 374 (3) (2016) 223–232.
[16] L. Ngo, M. Haas, Z. Qu, S.S. Li, J. Zenker, K.S. Teng, J.M. Gunnersen, M. Breuss, M. Habgood, D.A. Keays, J.I. Heng, TUBB5 and its disease-associated mutations influence the terminal differentiation and dendritic spine densities of cerebral cortical neurons, Hum. Mol. Genet. 23 (19) (2014) 5147–5158.
[17] M. Breuss, T. Fritz, T. Gstrein, K. Chan, L. Ushakova, N. Yu, F.W. Vonberg, B. Werner, U. Elling, D.A. Keays, Mutations in the murine homologue of TUBB5 cause microcephaly by perturbing cell cycle progression and inducing p53-associated apoptosis, Development 143 (7) (2016) 1126–1133.
[18] J.N. Pulvers, J. Bryk, J.L. Fish, M. Wilsch-Brauninger, Y. Arai, D. Schreier, R. Naumann, J. Helppi, B. Habermann, J. Vogt, R. Nitsch, A. Toth, W. Enard, S. Paabo, W.B. Huttner, Mutations in mouse Aspm (abnormal spindle-like microcephaly associated) cause not only microcephaly but also major defects in the germline, Proc. Natl. Acad. Sci. U. S. A. 107 (38) (2010) 16595–16600.
[19] J.F. Chen, Y. Zhang, J. Wilde, K.C. Hansen, F. Lai, L. Niswander, Microcephaly disease gene Wdr62 regulates mitotic progression of embryonic neural stem cells and brain size, Nat. Commun. 5 (2014) 3885.
[20] S.B. Lizarraga, S.P. Margossian, M.H. Harris, D.R. Campagna, A.P. Han, S. Blevins, R. Mudbhary, J.E. Barker, C.A. Walsh, M.D. Fleming, Cdk5rap2 regulates centrosome function and chromosome segregation in neuronal progenitors, Development 137 (11) (2010) 1907–1917.
[21] M. Trimborn, M. Ghani, D.J. Walther, M. Dopatka, V. Dutrannoy, A. Busche, F. Meyer, S. Nowak, J. Nowak, C. Zabel, J. Klose, V. Esquitino, M. Garshasbi, A.W. Kuss, H.H. Ropers, S. Mueller, C. Poehlmann, I. Gavvovidis, D. Schindler, K. Sperling, H. Neitzel, Establishment of a mouse model with misregulated chromosome condensation due to defective Mcph1 function, PLoS One 5 (2) (2010) e9242.
[22] G. Novarino, P. El-Fishawy, H. Kayserili, N.A. Meguid, E.M. Scott, J. Schroth, J.L. Silhavy, M. Kara, R.O. Khalil, T. Ben-Omran, A.G. Ercan-Sencicek, A.F. Hashish, S.J. Sanders, A.R. Gupta, H.S. Hashem, D. Matern, S. Gabriel, L. Sweetman, Y. Rahimi, R.A. Harris, M.W. State, J.G. Gleeson, Mutations in BCKD-kinase lead to a potentially treatable form of autism with epilepsy, Science 338 (6105) (2012) 394–397.
[23] N. Akizu, V. Cantagrel, J. Schroth, N. Cai, K. Vaux, D. McCloskey, R.K. Naviaux, J. Van Vleet, A.G. Fenstermaker, J.L. Silhavy, J.S. Scheliga, K. Toyama, H. Morisaki, F.M. Sonmez, F. Celep, A. Oraby, M.S. Zaki, R. Al-Baradie, E.A. Faqeih, M.A. Saleh, E. Spencer, R.O. Rosti, E. Scott, E. Nickerson, S. Gabriel, T. Morisaki, E.W. Holmes, J.G. Gleeson, AMPD2 regulates GTP synthesis and is mutated in a potentially treatable neurodegenerative brainstem disorder, Cell 154 (3) (2013) 505–517.
[24] M.T. Acosta, C.E. Bearden, F.X. Castellanos, L. Cutting, Y. Elgersma, G. Gioia, D.H. Gutmann, Y.S. Lee, E. Legius, M. Muenke, K. North, L.F. Parada, N. Ratner, K. Hunter-Schaedle, A.J. Silva, The Learning Disabilities Network (LeaDNet): using neurofibromatosis type 1 (NF1) as a paradigm for translational research, Am. J. Med. Genet. A 158A (9) (2012) 2225–2232.
[25] D. Ehninger, A.J. Silva, Rapamycin for treating Tuberous sclerosis and Autism spectrum disorders, Trends Mol. Med. 17 (2) (2011) 78–87.
[26] C. Contet, J.N. Rawlins, R.M. Deacon, A comparison of 129S2/SvHsd and C57BL/6JOlaHsd mice on a test battery assessing sensorimotor, affective and cognitive behaviours: implications for the study of genetically modified mice, Behav. Brain. Res. 124 (1) (2001) 33–46.
[27] P.L. Oliver, D.A. Keays, K.E. Davies, Behavioural characterisation of the robotic mouse mutant, Behav. Brain. Res. 181 (2) (2007) 239–247.
[28] A. Edwards, C.D. Treiber, M. Breuss, R. Pidsley, G.J. Huang, J. Cleak, P.L. Oliver, J. Flint, D.A. Keays, Cytoarchitectural disruption of the superior colliculus and an enlarged acoustic startle response in the Tuba1a mutant mouse, Neuroscience 195 (2011) 191–200.
[29] R. Paylor, J.N. Crawley, Inbred strain differences in prepulse inhibition of the mouse startle response, Psychopharmacology (Berl.) 132 (2) (1997) 169–180.
[30] J.L. Silverman, M. Yang, C. Lord, J.N. Crawley, Behavioural phenotyping assays for mouse models of autism, Nat. Rev. Neurosci. 11 (7) (2010) 490–502.
[31] Z.R. Donaldson, R. Hen, From psychiatric disorders to animal models: a bidirectional and dimensional approach, Biol. Psychiatry 77 (1) (2015) 15–21.
[32] R. Paylor, S. Hirotsune, M.J. Gambello, L. Yuva-Paylor, J.N. Crawley, A. Wynshaw-Boris, Impaired learning and motor behavior in heterozygous Pafah1b1 (Lis1) mutant mice, Learn. Mem. 6 (5) (1999) 521–537.
[33] J. Germain, E. Bruel-Jungerman, G. Grannec, C. Denis, G. Lepousez, B. Giros, F. Francis, M. Nosten-Bertrand, Doublecortin knockout mice show normal hippocampal-dependent memory despite CA3 lamination defects, PLoS One 8 (9) (2013) e74992.
[34] M. Nosten-Bertrand, C. Kappeler, C. Dinocourt, C. Denis, J. Germain, F. Phan Dinh Tuy, S. Verstraeten, C. Alvarez, C. Metin, J. Chelly, B. Giros, R. Miles, A. Depaulis, F. Francis, Epilepsy in Dcx knockout mice associated with discrete lamination defects and enhanced excitability in the hippocampus, PLoS One 3 (6) (2008) e2473.
[35] D. Wang, J.M. Pascual, H. Yang, K. Engelstad, X. Mao, J. Cheng, J. Yoo, J.L. Noebels, D.C. De Vivo, A mouse model for Glut-1 haploinsufficiency, Hum. Mol. Genet. 15 (7) (2006) 1169–1179.
[36] J.A. Obeso, M.C. Rodriguez-Oroz, M. Stamelou, K.P. Bhatia, D.J. Burn, The expanding universe of disorders of the basal ganglia, Lancet 384 (9942) (2014) 523–531.

[37] F.A. Middleton, P.L. Strick, Basal ganglia and cerebellar loops: motor and cognitive circuits, Brain. Res. Brain Res. Rev. 31 (2–3) (2000) 236–250.
[38] F.A. Middleton, P.L. Strick, Basal ganglia output and cognition: evidence from anatomical, behavioral, and clinical studies, Brain Cogn. 42 (2) (2000) 183–200.
[39] D.L. Braff, M.A. Geyer, Sensorimotor gating and schizophrenia. Human and animal model studies, Arch. Gen. Psychiatry 47 (2) (1990) 181–188.
[40] P.A. Arguello, J.A. Gogos, Modeling madness in mice: one piece at a time, Neuron 52 (1) (2006) 179–196.
[41] S.B. Powell, X. Zhou, M.A. Geyer, Prepulse inhibition and genetic mouse models of schizophrenia, Behav. Brain. Res. 204 (2) (2009) 282–294.
[42] S.J. Clapcote, T.V. Lipina, J.K. Millar, S. Mackie, S. Christie, F. Ogawa, J.P. Lerch, K. Trimble, M. Uchiyama, Y. Sakuraba, H. Kaneda, T. Shiroishi, M.D. Houslay, R.M. Henkelman, J.G. Sled, Y. Gondo, D.J. Porteous, J.C. Roder, Behavioral phenotypes of Disc1 missense mutations in mice, Neuron 54 (3) (2007) 387–402.
[43] A.H. Wong, S.A. Josselyn, Caution when diagnosing your mouse with schizophrenia: the use and misuse of model animals for understanding psychiatric disorders, Biol. Psychiatry 79 (1) (2016) 32–38.
[44] M.S. Moehle, R.F. Luduena, V. Haroutunian, J.H. Meador-Woodruff, R.E. McCullumsmith, Regional differences in expression of β-tubulin isoforms in schizophrenia, Schizophr. Res. 135 (1–3) (2012) 181–186.
[45] S.V. Haijma, N. Van Haren, W. Cahn, P.C. Koolschijn, H.E. Hulshoff Pol, R.S. Kahn, Brain volumes in schizophrenia: a meta-analysis in over 18 000 subjects, Schizophr. Bull. 39 (5) (2013) 1129–1138.
[46] V. Kumari, T. Sharma, Effects of typical and atypical antipsychotics on prepulse inhibition in schizophrenia: a critical evaluation of current evidence and directions for future research, Psychopharmacology (Berl.) 162 (2) (2002) 97–101.
[47] J.B. Manent, Y. Wang, Y. Chang, M. Paramasivam, J.J. LoTurco, Dcx reexpression reduces subcortical band heterotopia and seizure threshold in an animal model of neuronal migration disorder, Nat. Med. 15 (1) (2009) 84–90.
[48] J.B. Schulz, M. Weller, M.A. Moskowitz, Caspases as treatment targets in stroke and neurodegenerative diseases, Ann. Neurol. 45 (4) (1999) 421–429.
[49] X. Jiang, L. Li, Z. Ying, C. Pan, S. Huang, L. Li, M. Dai, B. Yan, M. Li, H. Jiang, S. Chen, Z. Zhang, X. Wang, A small molecule that protects the integrity of the electron transfer chain blocks the mitochondrial apoptotic pathway, Mol. Cell 63 (2) (2016) 229–239.
[50] M. Breuss, J. Morandell, S. Nimpf, T. Gstrein, M. Lauwers, T. Hochstoeger, A. Braun, K. Chan, E.R. Sanchez Guajardo, L. Zhang, M. Suplata, K.G. Heinze, K. Elsayad, D.A. Keays, The expression of tubb2b undergoes a developmental transition in murine cortical neurons, J. Comp. Neurol. 523 (15) (2015) 2161–2186.